Journal of Materials Chemistry

Cite this: *J. Mater. Chem.*, 2012, **22**, 21917

www.rsc.org/materials

PAPER

Highly enhanced performance of glucose biosensor *via in situ* growth of oriented Au micro-cypress

Zhenyu Chu, Lei Shi, Lifang Liu, Yu Liu and Wanqin Jin*

Received 16th August 2012, Accepted 5th September 2012
DOI: 10.1039/c2jm35554j

High sensitivity and accuracy are strongly required for biosensors due to their special application in the life and health of humans. In order to greatly enhance the above two parameters of the prepared biosensor, the architectures of Prussian blue and Au were purposefully designed. A single layer of PB grid with tight nano-holes was constructed to serve as a mould for the constraint of further Au deposition. Based on the steric hindrance effect, the Au crystal can be pushed towards one direction to *in situ* form a shape of a micro-cypress. Under a very low operation potential, −0.05 V, this composite film has been confirmed to own excellent abilities of performance enhancement and anti-interference as a glucose biosensor. This synthesis strategy can be expected to provide inspiration for morphology control of materials and high performance development of biosensors.

Introduction

Biosensors are a hot scientific field arousing many research passions because of their close relation with human health and safety.[1] Owing to their special application fields, sensitivity and accuracy are two essential parameters of biosensors for actual detection. Currently, the performance of a single material has hardly already been satisfied. Therefore, a common strategy of sensitivity improvement is the introduction of another electrochemically sensitive substance, such as a semi-conductor, metal or hybrid material.[2] However, in composite materials it is much more difficult than in single materials to obtain a regular film morphology due to the mismatching of properties and crystallization rate although structure control can obviously enhance the performance.[3] In terms of electrocatalysis, an oriented structure is an effective shape to improve performance because of its donation of fast electron transfer path and excellent catalytic abilities.[4] Accordingly, if an extra oriented material of good electrocatalytic activity can be grown on the original film surface, a great performance improvement can be expected. While for a single substance, orientation is really hard to be realized on account of the constriction of its whole growth dimensions.[5]

Prussian blue (PB) is an excellent electron mediator with the ability of potential decrease in electrochemical systems.[6] This advantage can promise the accuracy of prepared biosensors. Gold (Au) is a traditional but highly relevant electrode modifying material with outstanding catalytic activity.[7] Nevertheless, its free growth will tend to uniform extension in all directions until it reaches a large size,[8] and the application of Au modified electrodes often requires a quite high potential in physiological detection.[9] However, in actual detection systems, such a complex composition will easily produce a redox signal under a high potential to affect the analytical accuracy. Thus, if PB can play the role of a guide with a smart architecture to constrict the Au growth for orientation, the composite film will own both high sensitivity and accuracy.

Here, we adopted a single grid structure of PB with 250 nm thickness on a gold substrate as a mold to restrict the plane growth of Au. Au was limited to only grow towards the altitude direction to *in situ* form a micro-cypress morphology. Through silane modification of the Au surface, glucose oxidase was immobilized to produce a glucose biosensor. Under a very low potential of −0.05 V, the as-prepared biosensor exhibited an ultra-sensitive performance with an excellent anti-interference ability. This strategy of performance enhancement can provide a new inspiration in the morphology control of materials and the prepared biosensor owns a broadened application in the electrochemical analysis of more substances.

Experimental

Reagents and apparatus

Polystyrene latex microspheres (PS, 500 nm, 2.5 wt%) and $HClO_4$ (70 wt%) were purchased from Alfa-Aesar company. $K_4[Fe(CN)_6]\cdot 3H_2O$ (Sigma-Aldrich), $FeCl_3\cdot 6H_2O$ (Sigma-Aldrich), $HAuCl_4$ (Sigma-Aldrich), (3-glycidyloxypropyl) trimethoxysilane (GS) (Sigma-Aldrich), sodium *n*-dodecyl sulfate (Alfa-Aesar), glucose (Sinopharm Chemical Reagent Co., Ltd, China) were of analytical grade purity and used without further purification. 5 mg glucose oxidase (GOD, EC 1.1.3.4, 168 800

State Key Laboratory of Materials-Oriented Chemical Engineering, College of Chemistry and Chemical Engineering, Nanjing University of Technology, 5 Xinmofan Road, Nanjing 210009, P. R. China. E-mail: wqjin@njut.edu.cn; Fax: +86 25-8317-2292; Tel: +86 25-8317-2266

units g^{-1}, from Aspergillus niger, Sigma-Aldrich) was dispersed in 1500 μL 0.05 phosphate buffer solution with 0.1 M KCl (PBS, pH = 6.5) and was sufficient for the preparation of three electrodes. All solutions were prepared with deionized water.

The electrochemical properties were studied using an electrochemical workstation (CHI 660C, Shanghai Chenhua, China). All cyclic voltammetry (CV) experiments were operated in PBS at 25 °C. Pt wire and Ag/AgCl were used as the counter and reference electrodes, respectively. The scan rate was 50 mV s^{-1}. The images were collected in contact mode. Scanning electron microscopy employed a JEOL JSM-6390LV with a SC7620 Mini Sputter Coater from Quorum Technologies and EDX for elemental identification. Contact angle detection was characterized by a dropmeter (A100P, MAIST Inspection & Measurement Co. Ltd., China).

Preparation of PB single grid layer

A clean and bare Au electrode served as the substrate for film deposition. Firstly, one or two drops of polystyrene (PS) beads were added on the electrode surface to cover the whole Au area. The electrode was held stationary for 1 min. Secondly, the substrate was slowly immersed into deionized water and one or two droplets of 2% sodium *n*-dodecyl sulfate was dropped into this water in order to form a PS monolayer. Subsequently, the prepared PS monolayer modified electrode was lifted out of the trough and dried in the oven at 60 °C for 30 min in order to fix the beads to the surface.

When the deposition of the PS monolayer was complete, the electrode was then modified with PB using a self-assembly approach as in our previous work.[10] After 40 deposition cycles were finished, the electrode was washed and dried in the oven at 60 °C for 30 min. Finally, the prepared electrode was immersed in toluene for 4 h to remove the PS template and obtain a single layer of PB grid.

Oriented growth of Au

24 mM $HAuCl_4$ containing 1.2 M $HClO_4$ was prepared as the electrodeposition solution. The prepared PB modified electrode, Pt wire, and Ag/AgCl with saturated KCl solution served as work, counter and reference electrodes, respectively for deposition. The work electrode was kept vertical in the solution. Under 0.2 V, the deposition step was finished when the total electric quantity reached 2×10^{-2} C. Subsequently, the deposited PB–Au electrode was washed with deionized water and dried at 60 °C for 30 min.

Immobilization of glucose oxidase

The prepared electrode was immersed into 69% HNO_3 for 5 min to hydroxylate the Au surface. Then the electrode was cleaned and dipped into 2% (3-glycidyloxypropyl) trimethoxysilane (GS) at 37 °C for 1 h. The excess liquid was removed from the electrode surface and allowed to dry at 60 °C for 30 min. Finally, the electrode was immersed into the enzyme solution for 3 h in order to allow enzyme binding. Finally the electrode was washed using deionized water and stored at 4 °C.

Results and discussion

Growth process of Au cypress

In terms of electrocatalysis, a large surface area of film means a high electrochemical activity.[11] Also, for the immobilization of enzymes, it can provide more combination sites for bonding. Big crystals often cause a strong steric hindrance.[12] Based on this principle, we intended to produce a tight mold for Au growth in which is possible to constrain the accumulation towards planar directions. Accordingly, as we expected, a single layer of PB grid with 500 nm cavities was pre-formed on the gold substrate as an Au growth template (Fig. 1(a)). Then, the electrodeposition approach was employed to grow Au because of its rapid rate and large formation size of crystals. Whether the Au crystal will realize the oriented structure can be characterized by the microscopy technique. From the cross section image of the Au deposited electrode (the inset of Fig. 1(b)), we can find that on the substrate surface some isolated cypress-like Au crystals with 6 μm height were observed to be upright. Although this formation route is capable of obtaining the oriented Au structure, the morphology evolution should be further studied to clarify the orientation mechanism.

Growth evolution of film morphology

Electric quantity is a key parameter in the electrodeposition approach which could affect the thickness and morphology of the prepared film. Three samples of Au deposited electrodes with different applied electric quantities were prepared for characterization. Fig. 2(a)–(c) exhibit the surface morphologies of Au films formed by 1.0×10^{-2}, 1.5×10^{-2} and 2.0×10^{-2} C, respectively. The FESEM results (Fig. 2(a)) illustrate that Au particles will first fill into the cavities of the PB grid at the initial deposition. During this stage, the boundary of the PB walls can still be distinguished and the surface of Au is smooth. It seems that Au has a tendency to enter into the holes instead of covering the PB surface. This is because our prepared PB grid is hollow to expose the substrate material.[10] In this case, under the deposition potential, reduced Au from $HAuCl_4$ will prefer to accumulate into the cavities by Au–Au metallic bonds. With the prolonging

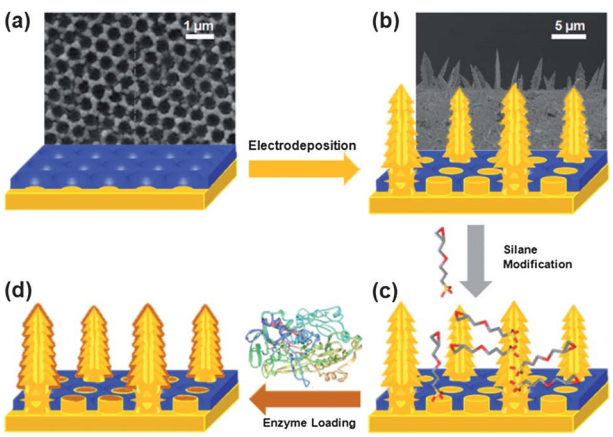

Fig. 1 The preparation scheme of the micro-cypress Au based biosensor. The insets of (a) and (b) are FESEM images of the PB grid covered electrode and cross section view of the Au deposited electrode.

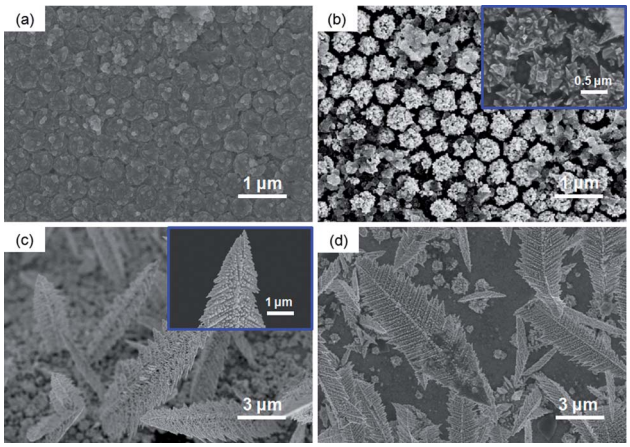

Fig. 2 The FESEM images of Au modified electrodes with different deposition electric quantity: (a) 1.0×10^{-2} C; (b) 1.5×10^{-2} C; (c) 2.0×10^{-2} C. The insets of (b) and (c) are the magnified images for partial film surface and tip view of single Au micro-cypress, respectively. (d) is the surface morphology of Au modified electrode without the template of PB grid.

of deposition time, on some sites, Au particles grew higher than before but not obviously larger in the plane directions (Fig. 2(b)). At this stage, the particle surface is no longer smooth, but consists of needle structures. That's because it is no longer limited by the PB walls at this altitude. In this case, Au was able to grow towards any directions. But owing to the over-tight distribution of the bottom Au particles, on the *xy* plane, the growth should meet strong resistance. Instead, the elevation towards the *z* direction is much easier. Therefore, some areas already appeared to have defects due to the slow accumulation of Au along the plane (Fig. 2(b)). When continuously increasing the Au amount, the rapid crystallization only functioned on an isolated location of the film (Fig. 2(c)). The cypress-like Au crystals were formed apart on the electrode surface. The crystal's shape owns many sharp edges like a knife and the surface is covered by *ca.* 50 nm nano-particles. This structure has the advantages of a large surface area and high solution coverage because of the separate distribution,[13] thus, it can be expected to own good performance of electrocatalysis. However, if the PB grid was not pre-prepared on the substrate as a template, the architecture of Au would be quite different. As shown in Fig. 2(d), without the plane constraint from PB, the crystal preferred to extend along the electrode surface. Its size can reach more than 20 μm length which is triple the value of film using the PB grid. Furthermore, not all the space contained Au in this way, most of the area presents itself to be blank exposing the substrate electrode. Consequently, the layer of PB grid can strongly confine the direction and size of the Au structure according to the purposeful tightness of space distribution for Au growth.

Electrochemical properties of the Au cypress-like film

In order to investigate the influence of the deposited Au cypress on the electrochemical properties, we compared the CV results of the PB grid modified electrodes before and after Au deposition. Obviously, the sharpness of CV current and the difference potential value of the two redox peaks have changed. The width of each peak narrowed and the height increased with the deposition of Au on the surface. This illustrates the electron transfer rate increases in both the oxidation and reduction processes. The peak difference values were calculated as 0.112 and 0.068 V for electrodes without and with Au deposited, respectively. Commonly, a lower value shows a weaker film resistance for redox electron transport and this reaction is more close to a reversible process. The above evidences revealed that the addition of Au on the electrode can promote the electrochemical ability of the film. This could be attributed to the packing into the cavities of the PB grid. Originally, electrons are only allowed to pass through the PB walls. Au is an excellent conductive material, thereby, the introduction of filled Au can provide the extra path and large area for movement of electrons.

For more clarity, an EIS experiment served as a quantifiable judgment of the impedance change of the prepared films. In order to display real properties, while performance in detection, this characterization was operated in buffer solution. As shown in Fig. 3(b), testing data of both the PB grid and Au deposited electrodes were further simulated by the equivalent circuit. We can find that the fitting line nearly matches the original data to

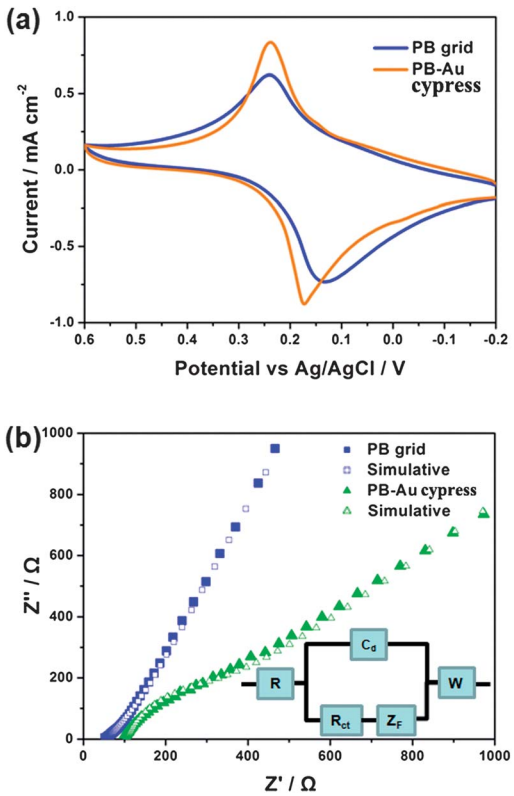

Fig. 3 Electrochemical characterizations of prepared PB grid modified electrode and Au cypress deposited electrode. (a) CV scanning diagrams. (b) Electrochemical impedance spectroscopy (EIS) experimental results. ■ and ▲ are experimental data. □ and △ are simulative data according to equivalent circuit. The inset is the equivalent circuit. C_d and R_{ct} are the double layer capacitance and the charge transfer resistance at the substrate electrode and film interface. R_s is the ohmic resistance of a solution plus a substrate. Z_F is the film associated impedance. W is the Warburg impedance for balance of the buffer solution diffusion under low frequencies.

confirm the reliability of our constructed equivalent circuit. Among the impedances, R_{ct} is the interface resistance between the prepared film and substrate electrode which exhibits a degree of hindering of electron transfer across from the film to the gold substrate electrode. The calculated values of R_{ct} are 226.2 and 106.8 Ω for the PB grid only and PB–Au cypress modified electrodes, respectively. It corresponds with the above deduction on the improved function of electron transfer rate by the deposition of Au. Good conductivity is a prerequisite for electrocatalytic performance.

Performance characterization of glucose biosensor

As shown in Fig. 1, in order to combine with the enzyme, the Au film was modified by (3-glycidyloxypropyl) trimethoxysilane (GS). Using the bonding ability of GS between the enzyme and metal surface,[14] this step ensures only the Au surface will own the ability of enzyme immobilization. PB can be free of blocking from protein to directly reduce the H_2O_2 which is produced by the glucose oxidase covered Au. Chronoamperometry was applied to characterize the performance of the prepared glucose biosensor. The application of Au film in biosensors often requires high operation potential, normally above 0.3 V. Without erasing, the PB serves as a common template because it can significantly decrease the detection potential. In real detection systems, such as blood, high potential will surely cause interference signals from the oxidation of other compounds. Owing to the close relation with human health, biosensors must have high accuracy in target detection. Here, we imposed a very low potential of −0.05 V on the electrode to fulfil the performance characterization. In order to investigate the influence of the morphology, we also studied the biosensor in which Au was only filled in the PB cavities (the surface morphology is the same as Fig. 2(a)). Initially, while adding 0.1 mM glucose in buffer solution, the current signals of both biosensors rapidly take a step up and remain stable (Fig. 4(a)). But after 5 additions, the increase in current step became less and less for the hole-filled Au film. According to the fitted data of the inset of Fig. 4(a), the current response to more than 0.6 mM of glucose concentration cannot remain linear. Instead, until reaching 1 mM addition of glucose, the current step of the Au cypress still kept a stable increase. For exploring the reason for the above, the Michaelis–Menten constant K_M was further calculated to confirm the film affinity for the enzyme. The Lineweaver–Burk equation[15] is applied to fit the values of K_M:

$$\frac{1}{i_{ss}} = \frac{1}{i_{max}} + \frac{K_M}{i_{max}}\frac{1}{C} \quad (1)$$

where K_M is the Michaelis–Menten constant, C is the concentration of glucose in the detection system, i_{ss} is the steady state current with a glucose concentration of C, i_{max} is the maximum current under saturated glucose concentration.

The values were 1.48 mM and 5.38 mM for the Au cypress and hole-filled Au biosensors, respectively (Fig. 5(a)). This illustrated that the oxidase had strongly locked onto the Au cypress surface to keep the stability in detection. That could account for the larger exposed area of Au crystals to provide more combination sites for the enzyme. 1.48 mM was also much lower than most reported biosensors (Table 1). The sensitivities of the prepared

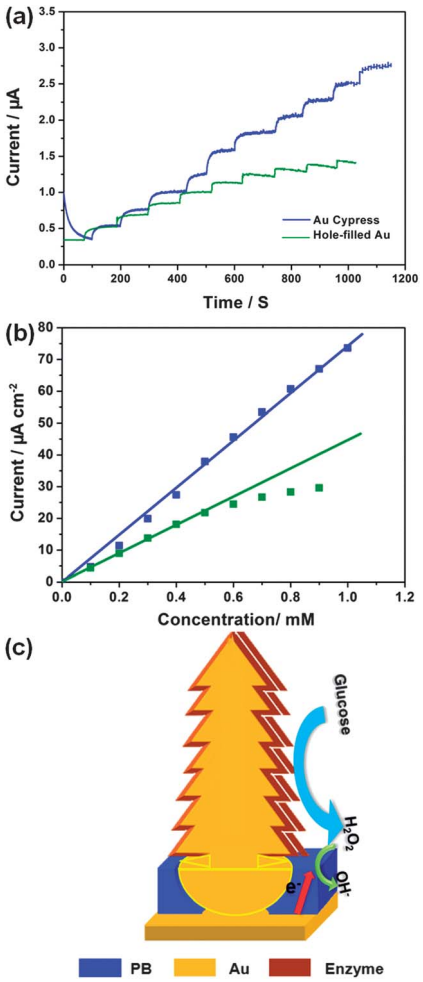

Fig. 4 (a) is the performance characterization results of the prepared cypress-like Au and only hole-filled Au film based biosensors in glucose detection; (b) is the fitting line according to the detection data; and (c) is the detection mechanism of the prepared biosensor.

glucose biosensors were analyzed according to the relations between response current and concentration of added glucose (the inset of Fig. 4(a)). The values were fitted as 74.2 and 44.7 μA mM cm^{-2} for cypress and hole-filled structures, respectively. If only applying PB grid film as a biosensor, the sensitivity was found to be 30.6 μA mM cm^{-2} in our previous work.[10] Consequently, we can conclude that: (1) the introduction of Au can increase the performance; (2) the morphology of the Au film is an important determinant to the sensitivity, linear arrangement and enzyme affinity of the prepared biosensors.

Mechanism of glucose detection

The excellent performance should be attributed to the special architecture of the prepared film. Commonly, the height of the catalytic film is often uniform with weak fluctuation and the difference between top and bottom is very small. In this case, the effective contact area with the solution is only the film plane. Our formed Au micro-cypresses are *ca.* 8 μm altitude away from the substrate.

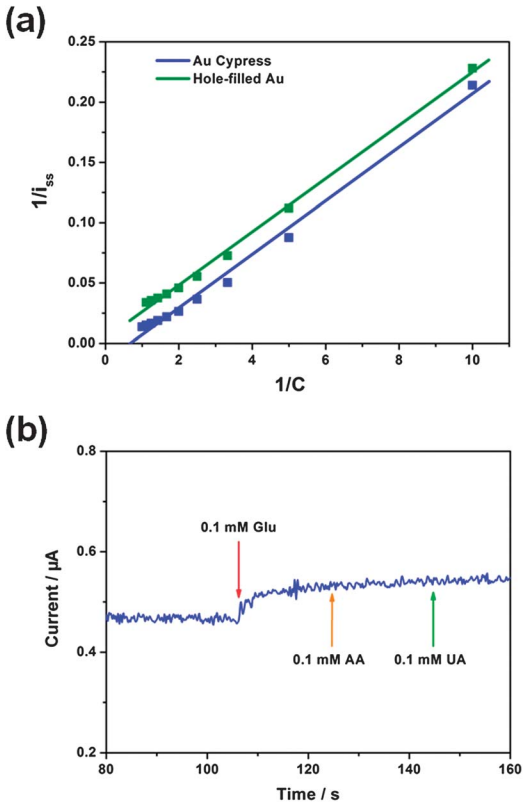

Fig. 5 (a) Diagram of the fitted Lineweaver–Burk equation according to the chronoamperometry data of Au-cypress and hole-filled Au based biosensors. (b) The anti-interference characterization of the prepared Au cypress-PB modified electrode.

Besides, they are distributed apart as many isolated micro-electrodes, therefore, the target solution can cover the whole surface of the Au crystal to obviously increase the electro-catalytic area. The above deduction can be confirmed by the comparison of the contact angle between the PB grid film and Au–PB film. The deposition of Au on the PB grid can enhance the hydrophilia from 83.9° to 52.5° which illustrated that the solution would more easily moisten the Au cypress architecture to improve the enzyme reaction (Fig. 6). Furthermore, the surface of each Au cypress consists of nano-particles and many edges. This is the second magnification of the catalytic area. After twice increasing the electrocatalysis, glucose can be fast oxidized to produce H_2O_2. Then the bottom PB can make the function of reduction to create a current signal that passes

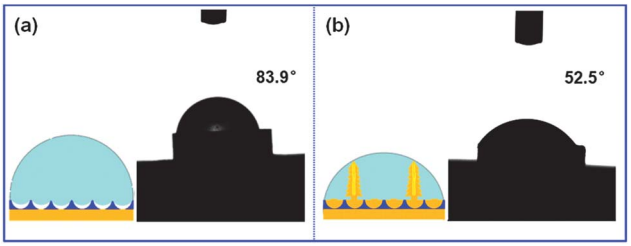

Fig. 6 The contact angle characterizations of electrodes modified by PB grid (a) and Au cypress–PB (b).

through itself to the electrode surface. If there is no such signal magnification, such as in the structure of hole-filled Au, the performance will decrease by half.

Compared with reported literature data, our prepared Au cypress structured biosensor owns not only higher sensitivity, but also operation potential that is much lower than other PB or Au film based electrodes (Table 1). This advantage of low potential can be exhibited by the outstanding anti-interference performance. As shown in Fig. 5(b), after the addition of 0.1 mM glucose, the same concentration of ascorbic acid and uric acid were respectively introduced into the detection system, but no obvious current signal change occurred. This is the prerequisite for the accuracy of the biosensor in real applications.

Conclusion

We have successfully designed and realized an oriented Au micro-cypressed structure by the assistance of a single layer PB grid. The tight distribution of growth cavities can constrain the Au accumulation towards the plane directions and cause it to only grow in one direction. This architecture has excellent electron conductivity and large electrocatalytic area. Under low operation potential, −0.05 V, the as-prepared biosensor can exhibit an ultra-sensitive response to glucose. In perspective, the oriented synthesis strategy can guide the morphology control of further materials and the design idea of performance enhancement can provide meaningful inspiration for the development of biosensors.

Acknowledgements

This work was supported by the National Basic Research Program of China (no. 2009CB623406), National Natural Science Foundation of China (no. 20990222 and 21176115).

Table 1 The performance comparison of literature reported glucose biosensors

Modified material	Applied potential (V)	Sensitivity (μA mM cm^{-2})	K_m (mM)	Ref.
Au cypress/PB grid	−0.05	74.3	1.48	This work
PMMA/BSA	0.4	44.1	19.2	16
ZnO nanotubes	0.8	21.7	19	17
PPyAA/Au	0.6	13.4	1.83	18
AuNPs/MWCNT	0.3	19.27	6.7	9*c*
PtAu/C	0.35	4.7	—	19
PB/POAP	0.6	44	22.8	20
PB/sol–gel	0	26.6	3.76	21

Notes and references

1 (*a*) K. Campbell, S. A. Haughey, H. Top, H. Egmond, N. Vilarino, L. M. Botana and C. T. Elliott, *Anal. Chem.*, 2010, **82**, 2977–2988; (*b*) Y. Peng, X. Wang, Y. Xiao, L. Feng, C. Zhao, J. Ren and X. Qu, *J. Am. Chem. Soc.*, 2009, **131**, 13813–13818.

2 (*a*) N. Lavanya, S. Radhakrishnan and C. Sekar, *Biosens. Bioelectron.*, 2012, **36**, 41–47; (*b*) N. Q. Dung, D. Patil, Y. Duong, H. Jung and D. Kim, *Sens. Actuators, B*, 2012, **166**, 103–109; (*c*) Y. Won, D. Aboagye, H. S. Jang, A. Jitianu and L. A. Stanciu, *J. Mater. Chem.*, 2010, **20**, 5030–5034.

3 (*a*) V. Vamvakaki, K. Tsagaraki and N. Chaniotakis, *Anal. Chem.*, 2006, **78**, 5538–5542; (*b*) N. Bu, C. Tang, X. He and X. Yin, *Chem. Commun.*, 2011, **47**, 7689–7691; (*c*) J. C. Claussen, A. D. Franklin, A. Haque, D. M. Porterfield and T. S. Fisher, *ACS Nano*, 2009, **3**, 37–44.

4 (*a*) G. Reguera, K. D. McCarthy, T. Mehta, J. S. Nicoll, M. T. Tuominen and D. R. Lovley, *Nature*, 2005, **435**, 1098–1101; (*b*) J. R. Jennings, A. Ghicov, L. M. Peter, P. Schmuki and A. B. Walker, *J. Am. Chem. Soc.*, 2008, **130**, 13364–13372.

5 (*a*) K. Mun, S. D. Alvarez, W. Choi and M. J. Sailor, *ACS Nano*, 2010, **4**, 2070–2076; (*b*) G. Liu, C. Thomas, G. S. W. Craig and P. F. Nealey, *Adv. Funct. Mater.*, 2010, **20**, 1251–1257; (*c*) S. Feng, X. Xiong, G. Zhang, N. Xia, Y. Chen and W. Wang, *Macromolecules*, 2009, **42**, 281–287.

6 (*a*) W. Zhao, J. Xu, C. Shi and H. Chen, *Langmuir*, 2005, **21**, 9630–9634; (*b*) Z. Y. Chu, Y. N. Zhang, X. L. Dong, W. Q. Jin, N. P. Xu and B. Tieke, *J. Mater. Chem.*, 2010, **20**, 7815–7820.

7 (*a*) N. Jha and S. Ramaprabhu, *Nanoscale*, 2010, **2**, 806–810; (*b*) H. Zhong, X. Lei, X. Hun and S. Zhang, *Chem. Commun.*, 2009, 6958–6960.

8 L. Wang, S. Guo, X. Hu and S. Dong, *Electrochem. Commun.*, 2008, **10**, 95–99.

9 (*a*) B. Haghighi, S. Bozorgzadeh and L. Gorton, *Sens. Actuators, B*, 2011, **155**, 577–583; (*b*) F. Wang, Y. Wang, K. Lu, X. Wei and B. Ye, *J. Electroanal. Chem.*, 2012, **674**, 83–89; (*c*) P. Si, P. Kannan, L. Guo, H. Son and D. Kim, *Biosens. Bioelectron.*, 2011, **26**, 3845–3851.

10 Z. Y. Chu, L. Shi, Y. N. Zhang, W. Q. Jin, S. Warren and E. Dempsey, *J. Mater. Chem.*, 2012, **22**, 14874–14879.

11 (*a*) M. N. Zhang, Y. M. Yan, K. P. Gong, L. Q. Mao, Z. X. Guo and Y. Chen, *Langmuir*, 2004, **20**, 8781–8785; (*b*) W. Sugimoto, H. Iwata, Y. Yasunaga, Y. Murakami and Y. Takasu, *Angew. Chem., Int. Ed.*, 2003, **42**, 4092–4096.

12 (*a*) E. Colas, D. E. Aspnes, R. Bhat, A. A. Studna, J. P. Harbison, L. T. Florez, M. A. Koza and V. G. Keramidas, *J. Cryst. Growth*, 1991, **107**, 47–55; (*b*) S. Yokoyama, H. Goto, T. Miyamoto, N. Ikeda and K. Shibahara, *Appl. Surf. Sci.*, 1997, **112**, 75–81.

13 A. A. Karyakin, E. A. Puganova, I. A. Bolshakov and E. E. Karyakina, *Angew. Chem., Int. Ed.*, 2007, **46**, 7678–7680.

14 M. J. Song, D. H. Yun and S. I. Hong, *Biosci., Biotechnol., Biochem.*, 2009, **73**, 474–478.

15 R. Kamln and G. Wilson, *Anal. Chem.*, 1980, **52**, 1198–1205.

16 C. X. He, J. H. Liu, Q. L. Zhang and C. Wu, *Sens. Actuators, B*, 2012, **166**, 802–808.

17 T. Kong, Y. Chen, Y. P. Ye, K. Zhang, Z. X. Wang and X. Wang, *Sens. Actuators, B*, 2009, **138**, 344–350.

18 M. Senel and C. Nergiz, *Curr. Appl. Phys.*, 2012, **12**, 1118–1124.

19 B. Singh, F. Laffir, T. McCormac and E. Dempsey, *Sens. Actuators, B*, 2010, **150**, 80–92.

20 D. W. Pan, J. H. Chen, L. H. Nie, W. Y. Tao and S. Z. Yao, *Electrochim. Acta*, 2004, **49**, 795–801.

21 R. P. Liang, J. L. Jiang and J. D. Qiu, *Electroanalysis*, 2008, **20**, 2642–2648.

